Radiation Protection Dosimetry (2017), Vol. 177, No. 3, pp. 261–271
Advance Access publication 7 April 2017
doi:10.1093/rpd/ncx039

# A COMPARATIVE STUDY OF THE DOSIMETRIC FEATURES OF α-$Al_2O_3$:C,Mg AND α-$Al_2O_3$:C

J.M. Kalita and M.L. Chithambo*
Department of Physics and Electronics, Rhodes University, P O Box 94, Grahamstown 6140, South Africa

*Corresponding author: m.chithambo@ru.ac.za

*Received 20 December 2016; revised 2 March 2017; editorial decision 3 March 2017; accepted 14 March 2017*

**A comparative study of the dosimetric features of α-$Al_2O_3$:C,Mg and α-$Al_2O_3$:C relevant to thermoluminescence dosimetry is reported. A glow curve of α-$Al_2O_3$:C,Mg measured at 1°C/s after beta irradiation to 1 Gy shows two subsidiary peaks at 42°C (labelled as I) and 72°C (II) and the main peak at 161°C (III) whereas a glow curve of α-$Al_2O_3$:C measured under the same conditions shows the main peak at 178°C (II′) and a lower intensity peak at 48°C (I′). Apart from these ones, there are several other peaks at temperatures beyond that of the main peak in both α-$Al_2O_3$:C,Mg and α-$Al_2O_3$:C. However, the latter are not included in this study. We report a comparative quantitative analysis of dose response and fading of peaks I, II and III of α-$Al_2O_3$:C,Mg and peaks I′ and II′ of α-$Al_2O_3$:C. Analysis shows that the dose response of peaks I and III is sublinear within 1–10 Gy whereas that of peak II is superlinear within 1–4 Gy followed by a sublinear region within 4–10 Gy. In comparison, the dose response of peak I′ is superlinear within 1–4 Gy followed by a sublinear region within 4–10 Gy whereas that of peak II′ is sublinear within 1–4 Gy followed by a superlinear region within 4–10 Gy. As regards to fading corresponding to 1 Gy, peak I is very unstable and fades within 300 s, peak II is more stable and takes up to 43200 s to fade. In comparison, peak III fades down to 30% of its initial intensity within 2400 s. Interestingly, between 2400 and 800 s, the intensity fades by 17% only. Regarding fading in α-$Al_2O_3$:C, peak I′ fades within 600 s whereas peak II′ shows an inverse fading behaviour up to 64800 s. The rate of fading for peaks I, II and III in α-$Al_2O_3$:C,Mg was found to decrease with increase in dose. However, no such behaviour was observed in α-$Al_2O_3$:C. The fading in both samples is discussed on the basis of a charge hopping mechanism.**

## INTRODUCTION

Carbon-doped aluminium oxide (α-$Al_2O_3$:C) is a supersensitive luminescent material widely used as a thermoluminescence (TL) and optically stimulated luminescence (OSL) dosimeter[1, 2]. The doping of carbon in $Al_2O_3$ promotes oxygen vacancies (F and $F^+$ centres) which are responsible for radiation sensitivity of α-$Al_2O_3$:C[3]. Research concerning the luminescence mechanisms as well as the dosimetric features of α-$Al_2O_3$:C has been carried out extensively[1–3]. Literature shows that although there are both F and $F^+$ centres in α-$Al_2O_3$:C, the main emission is due to the F centres characterised by an emission at 415 nm with a luminescence lifetime of ~35 ms[4–6].

Apart from α-$Al_2O_3$:C, $Al_2O_3$ doped with carbon and magnesium (α-$Al_2O_3$:C,Mg) is also a ultra-sensitive luminescent material developed for applications in optical data storage and imaging[7–9]. α-$Al_2O_3$:C,Mg contains a high concentration of F and $F^+$ centres as well as some aggregate defects, namely $F_2^{2+}$(2Mg), $F_2^{2+}$(Mg) and $F_2^{+}$(2Mg)[8]. Due to the presence of such luminescence centres, several emission peaks can be seen at 325, 415, 500, 510 and 750 nm[10]. The luminescence lifetime of an $F^+$ centre is ~7 ns[11] whereas that of the $F_2^{2+}$(2Mg) and $F_2^{+}$(2Mg) centres is <100 ns[12]. The presence of these short lifetime luminescence centres in α-$Al_2O_3$:C,Mg makes it a very sensitive and fast-responsive radiation dosimeter for application in 2D dose mapping and real-time optical fibre dosimetry.

Studies on luminescence features of α-$Al_2O_3$:C, Mg show that despite its use for optical data storage, it can be applied as a fluorescent nuclear track detector in the dosimetry of neutrons[13] as well as heavy charged particle and energetic protons[14]. Eller *et al.*[15] studied radio-photoluminescence (RPL) features of α-$Al_2O_3$:C,Mg under UV (335 nm) and red (615 nm) excitation. The RPL signal was found to exhibit a linear dose response under UV as well as red excitation[15]. Ahmed *et al.*[16] studied image reconstruction in 2D dosimetry using α-$Al_2O_3$:C and α-$Al_2O_3$:C,Mg by a laser scanning system. This analysis showed that due to the higher intensity of $F^+$ centre emission in α-$Al_2O_3$:C,Mg than in α-$Al_2O_3$:C, OSL images recorded from α-$Al_2O_3$:C,Mg need less correction for pixel bleeding that is common in laser scanning 2D dosimetry. Most recently, Kalita and Chithambo[17] reported TL features of α-$Al_2O_3$:C,Mg relevant to TL dosimetry. The dose response of the main glow peak was found to be superlinear within 0.1–30 Gy becoming sublinear thereafter up to 100 Gy. The TL was found to be well reproducible but it faded down to ~22%

of its initial value within 2400 s after irradiation and thereafter to ~14% within 64 800 s. The rate of fading was faster than would be acceptable for a dosimeter. It was speculated that the fading is due to the presence of shallow traps in the material[17].

In this work, we report the dosimetric features of the secondary peaks of α-$Al_2O_3$:C,Mg. However, for completeness, the same features for the main peak of α-$Al_2O_3$:C,Mg are also included. Further, a comparative study of the dosimetric features of α-$Al_2O_3$:C, Mg and α-$Al_2O_3$:C has been carried out to investigate the potential standard of α-$Al_2O_3$:C,Mg as a TL dosimeter.

## EXPERIMENTAL DETAILS

Samples used were α-$Al_2O_3$:C,Mg chips of size 5 × 2.5 × 1 $mm^3$ and α-$Al_2O_3$:C discs of diameter 5 mm and thickness 1 mm (Landauer, Inc; Oklahoma, USA). TL was measured using a RISØ TL/OSL DA-20 Luminescence Reader from a sample irradiated at ambient temperature using a $^{90}Sr/^{90}Y$ beta source at a nominal dose rate of 0.1028 Gy/s. The luminescence was detected by an EMI 9235QB photomultiplier tube through a 7 mm Hoya U-340 filter (transmission band 250–390 nm FWHM). All measurements were carried out in a nitrogen atmosphere to prevent spurious signals from air.

The dose response of α-$Al_2O_3$:C,Mg and α-$Al_2O_3$:C were studied within 1–10 Gy. In order to measure TL at extended doses, say 100 Gy, a neutral density filter is sometimes essential to attenuate the excessive luminescence intensity which is potentially hazardous for the photomultiplier tube. However, use of a neutral density filter has been found to not only reduce the intensity of a glow peak as desired but to also affect adversely the shape and position of the peak[17]. The measurement of a dose response curve from very low to very high doses thus produces two conflicting requirements for measurements on the same glow curve: to use a neutral density filter against very high dose signals but to also measure TL from secondary peaks where use of a neutral density filter is unnecessary. Therefore, to avoid the experimental artefact of change of shape and position of a peak caused by the presence of a neutral density filter, the dose response was studied only up to 10 Gy. On the other hand, to achieve adequate intensity for the secondary peaks, we preferred to study the dose response from 1 Gy.

To study fading of the peaks we used delays of 1, 10, 30, 60, 120, 300, 600, 1200, 2400, 4800, 9600, 18 000, 43 200 and 64 800 s between irradiation and measurement. During storage, the samples were kept in dark at room temperature ~25°C. To study the effect of irradiation dose on fading of the TL signal, the samples were irradiated to different doses (1, 2 and 4 Gy). Each measurement was repeated three times under identical conditions. The average of these three measurements was used for analysis.

## RESULTS AND DISCUSSION

### TL glow curves

Figure 1 shows glow curves of α-$Al_2O_3$:C,Mg and α-$Al_2O_3$:C recorded at 1°C/s after irradiation to different doses (1–10 Gy). In the glow curves of 1 Gy beta irradiated α-$Al_2O_3$:C,Mg, there are two secondary peaks at 42 and 72°C and a high intensity peak at 161°C, whereas in the glow curves of 1 Gy beta irradiated α-$Al_2O_3$:C, there is a secondary peak at 48°C and a high intensity peak at 178°C. The position of all glow peaks of α-$Al_2O_3$:C,Mg and the 48°C peak of α-$Al_2O_3$:C are independent of dose, whereas the position of the 178°C peak of α-$Al_2O_3$:C shifts towards lower temperature with dose. Kalita and Chithambo[18] reported that, for heating at 1°C/s, the glow curve of α-$Al_2O_3$:C,Mg consists of the main peak at 161°C, two lower temperature secondary peaks at 42 and 72°C before the main peak and four higher temperature secondary peaks at 193,

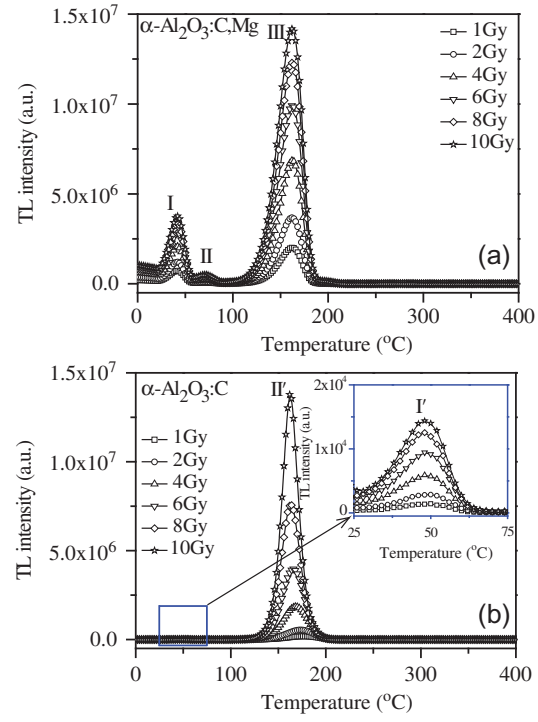


Figure 1. Glow curves of (**a**) α-$Al_2O_3$:C,Mg and (**b**) α-$Al_2O_3$:C recorded at 1°C/s after irradiation to different doses (1–10 Gy). The inset in (b) shows the magnified portion of the glow curves intended to show a secondary peak I′ of α-$Al_2O_3$:C.

279, 330, 370°C after the main peak. Regarding α-$Al_2O_3$:C, Chithambo and Seneza[19] found that the glow curve of α-$Al_2O_3$:C measured at 1°C/s consists of the main peak at 186°C, and secondary peaks at 46 and 314°C. Further investigation showed that apart from the 46°C and 314°C secondary peaks, the glow curve of α-$Al_2O_3$:C contains two other secondary peaks, one embedded within the main peak at its higher temperature end and the other, at above 400°C[20]. For ease of reference, the glow peaks of α-$Al_2O_3$:C,Mg at 42, 72, 161, 193, 279, 330 and 370°C are labelled as I, II, III, IV, V, VI and VII, respectively. On the other hand, the glow peaks of α-$Al_2O_3$:C appearing at 46, 178 and 314°C are labelled as I′, II′ and III′, respectively. Further, the secondary peak that is embedded within the main peak is labelled as IIB′ and the peak that appears above 400°C is labelled as IV′. In this labelling, peak III of α-$Al_2O_3$:C,Mg and peak II′ of α-$Al_2O_3$:C represent the main peak and all others, secondary peaks.

## Dose response

Kalita and Chithambo[17] studied the dose response of the main glow peak of α-$Al_2O_3$:C,Mg under beta irradiation. The response was found to be superlinear from 0.1 to 30 Gy and thereafter sublinear up to 100 Gy. In comparison, Yukihara *et al.*[21] and Chithambo[22] independently found that the dose response of the main glow peak of α-$Al_2O_3$:C under beta irradiation is linear within 1–10 Gy, superlinear up to 30 Gy and sublinear above 30 Gy.

In this work, we focus on the dose response of the secondary peaks I (at 42°C) and II (at 72°C) of α-$Al_2O_3$:C,Mg and peak I′ (at 48°C) of α-$Al_2O_3$:C. However, for completeness, the dose response of peak III (at 161°C) of α-$Al_2O_3$:C,Mg and peak II′ (at 178°C) of α-$Al_2O_3$:C are also reported.

Figure 2 shows the dose response of α-$Al_2O_3$:C,Mg and α-$Al_2O_3$:C. Figure 2a–c shows the variation of the peak intensity of peaks I, II and III of α-$Al_2O_3$:C, Mg with dose whereas Figure 2d and e shows the same feature for peaks I′ and II′ of α-$Al_2O_3$:C. For each dose, a data point in Figure 2a–e represents the average from three identical measurements. The error bars representing the standard deviation, are disguised by the size of the data points in Figure 2. For Figure 2a and c, where this applies, the fractional error is within 1.0–5.0% and 1.0–3.0%, respectively.

The dose response in all the examples shown could be well-described by an empirical cubic function $y(D)$ given by the following equation:

$$y(D) = k_0 + k_1 D + k_2 D^2 + k_3 D^3 \qquad (1)$$

where $k_0$, $k_1$, $k_2$ and $k_3$ are the constants. The same cubic function was also used to describe the X-ray dose response of calcite[23] as well as the beta dose response of the main peak of α-$Al_2O_3$:C,Mg[17]. The values of the constants corresponding to the dose response of each peak were determined after iteration to the best fit. In case of α-$Al_2O_3$:C,Mg, the constants for peak I are $k_0 = (1.99 \pm 0.45) \times 10^5$, $k_1 = (5.33 \pm 0.37) \times 10^5\ \mathrm{Gy}^{-1}$, $k_2 = -(1.36 \pm 0.79) \times 10^4\ \mathrm{Gy}^{-2}$ and $k_3 = -(4.18 \pm 4.71) \times 10^2\ \mathrm{Gy}^{-3}$; for peak II, $k_0 = (7.89 \pm 4.43) \times 10^3$, $k_1 = (5.12 \pm 0.37) \times 10^4\ \mathrm{Gy}^{-1}$, $k_2 = (1.46 \pm 0.78) \times 10^3\ \mathrm{Gy}^{-2}$ and $k_3 = -(1.58 \pm 0.46) \times 10^2\ \mathrm{Gy}^{-3}$; and for peak III, $k_0 = (3.44 \pm 0.13) \times 10^5$, $k_1 = (1.65 \pm 0.11) \times 10^6\ \mathrm{Gy}^{-1}$, $k_2 = (1.20 \pm 2.34) \times 10^4\ \mathrm{Gy}^{-2}$ and $k_3 = -(3.89 \pm 1.40) \times 10^3\ \mathrm{Gy}^{-3}$. On the other hand, in the case of α-$Al_2O_3$:C, the constants for peak I′ are $k_0 = (3.09 \pm 0.59) \times 10^2$, $k_1 = (9.75 \pm 0.49) \times 10^2\ \mathrm{Gy}^{-1}$, $k_2 = (1.45 \pm 0.10) \times 10^2\ \mathrm{Gy}^{-2}$ and $k_3 = -(1.03 \pm 0.06) \times 10^1\ \mathrm{Gy}^{-3}$; and for peak II′, $k_0 = -(7.42 \pm 5.26) \times 10^5$, $k_1 = (9.60 \pm 4.37) \times 10^5\ \mathrm{Gy}^{-1}$, $k_2 = -(1.57 \pm 0.92) \times 10^5\ \mathrm{Gy}^{-2}$ and $k_3 = (2.05 \pm 0.55) \times 10^4\ \mathrm{Gy}^{-3}$. Each solid line through data points in Figure 2a–e shows the best fit ($R^2 = 0.99$) of Eq. (1). In all the cases, the residuals, fluctuating about zero, signify that the function, $y(D)$ was a proper fit for the dose response and thus suitable for quantitative analysis.

For quantitative analysis of the dose response, the superlinearity index, $g(D) = [\{(D\,y''(D))/(y'(D))\} + 1]$, which gives an indication of the change in slope of the dose response[24, 25] has been used. In the expression, $y(D)$ is the analytical function that defines the exact behaviour of dose response, $y'(D)$ and $y''(D)$ are the first and second order derivatives of the function $y(D)$. A value of $g(D) > 1$ indicates a superlinear response, while $g(D) = 1$ signifies linear response and $g(D) < 1$ denotes sublinearity. Similarly, if $y''(D) > 0$, $y'(D)$ and $y(D)$ increases with dose $D$, $y(D)$ is then superlinear; if $y''(D) < 0$, $y'(D)$ decreases with $D$, $y(D)$ is then sublinear and if $y''(D) = 0$, $y'(D)$ is constant with $D$ then $y(D)$ is linear[24]. It should be noted that if the initial region of the dose response is linear then the supralinetity index $f(D)$ given by $f(D) = [\{y(D)/D\}/\{y(D_1)/D_1\}]$ (where, $D_1$ is normalised dose) can also be used to study the amount of deviation from the linearity of the dose response.

The dose response shown in Figure 2 is described in detail quantitatively in Figure 3. Figure 3a–c shows the variation of $y'(D)$ and $y''(D)$ with dose corresponding to peaks I, II and III of α-$Al_2O_3$:C, Mg whereas Figure 3d and e shows the same features but for peaks I′ and II′ of α-$Al_2O_3$:C. The inset in each figure shows the variation of $g(D)$ with dose for the corresponding peak. The conclusions for the analysis of dose response obtained from Figures 2 and 3 are as follows:

(i) For peak I of α-$Al_2O_3$:C,Mg (Figure 3a): $y'(D)$ decreases with $D$ and $y''(D) < 0$ within 1–10 Gy. Moreover, $g(D) < 1$ within 1–10 Gy. All this means that $y(D)$ is sublinear within 1–10 Gy.

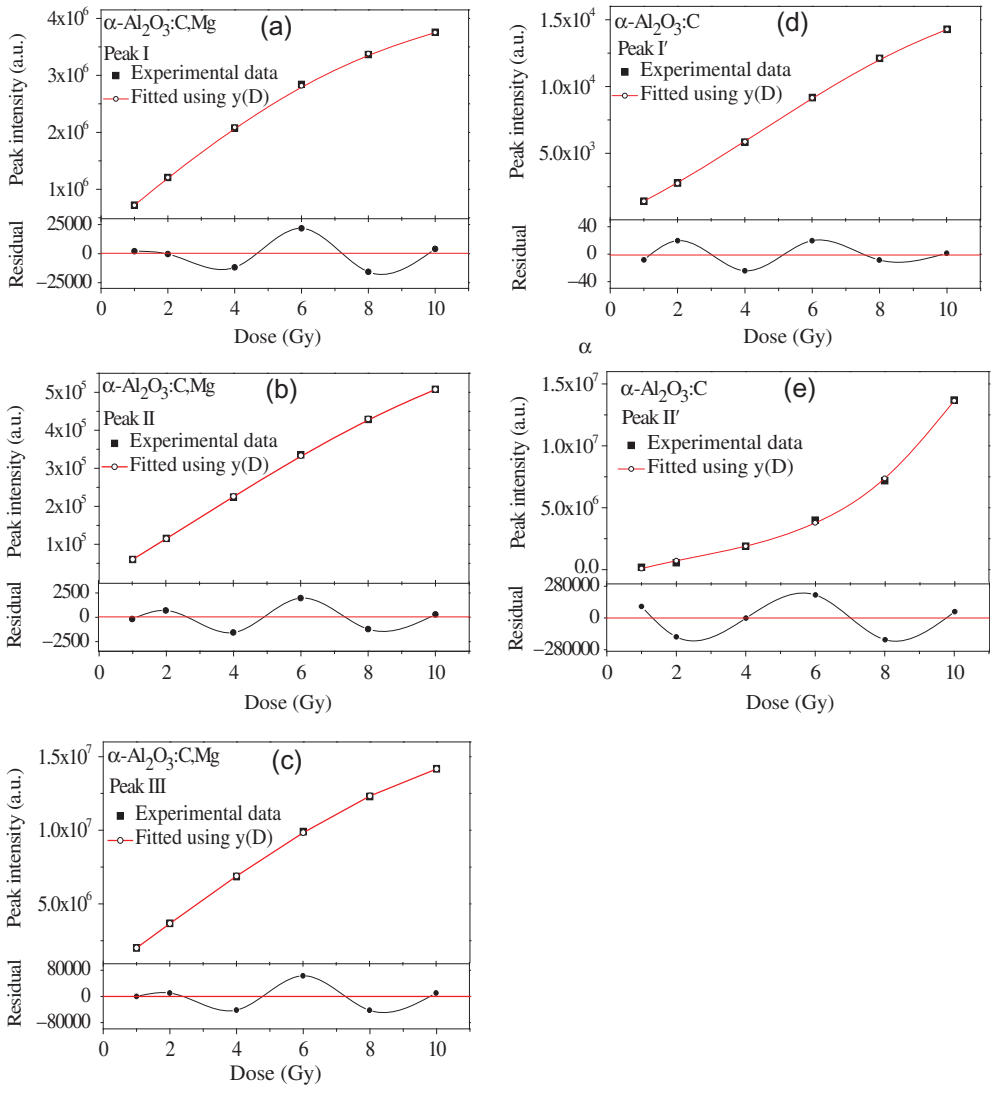


Figure 2. Dose response of peaks (**a**) I, (**b**) II and (**c**) III of α-$Al_2O_3$:C,Mg and in (**d**, **e**) for peaks I′ and II′ of α-$Al_2O_3$:C. The solid line through the data points in each case (squares) is the best fit of the function $y(D)$ given in Eq. 1. The residuals, confirming the goodness of fit, are shown for completeness.

(ii) For peak II of α-$Al_2O_3$:C,Mg (Figure 3b): $y'(D)$ as well as $y(D)$ increase with dose $D$ and $y''(D) > 0$ within 1–2 Gy. Also, $g(D) > 1$ within 1–2 Gy. The conclusion here is that $y(D)$ is superlinear within 1–2 Gy. Further, $y'(D)$ decreases with $D$ and $y''(D) < 0$ above 4–10 Gy. Moreover, $g(D) < 1$ within 4–10 Gy. These facts signify that $y(D)$ is sublinear within 4–10 Gy.

(iii) For peak III of α-$Al_2O_3$:C,Mg (Figure 3c): $y'(D)$ decreases with $D$ and $y''(D) < 0$ within 1–10 Gy. Moreover, $g(D) < 1$ within 1–10 Gy. All this means that $y(D)$ is sublinear within 1–10 Gy.

(iv) For peak I′ of α-$Al_2O_3$:C (Figure 3d): $y'(D)$ as well as $y(D)$ increase with dose $D$ and $y''(D) > 0$ within 1–4 Gy. Also, $g(D) > 1$ within 1–4 Gy. All this signifies that $y(D)$ is superlinear within 1–4 Gy. Further, $y'(D)$ decreases with $D$ and $y''(D) < 0$ above 4–10 Gy. Moreover, $g(D) < 1$ within 4–10 Gy. All these mean that $y(D)$ is sublinear within 4–10 Gy.

(v) For peak II′ of α-$Al_2O_3$:C (Figure 3e): $y'(D)$ decreases with $D$ and $y''(D) < 0$ within 1–2 Gy. Moreover, $g(D) < 1$ within 1–2 Gy. This means that $y(D)$ is sublinear within 1–2 Gy. Further, $y'$

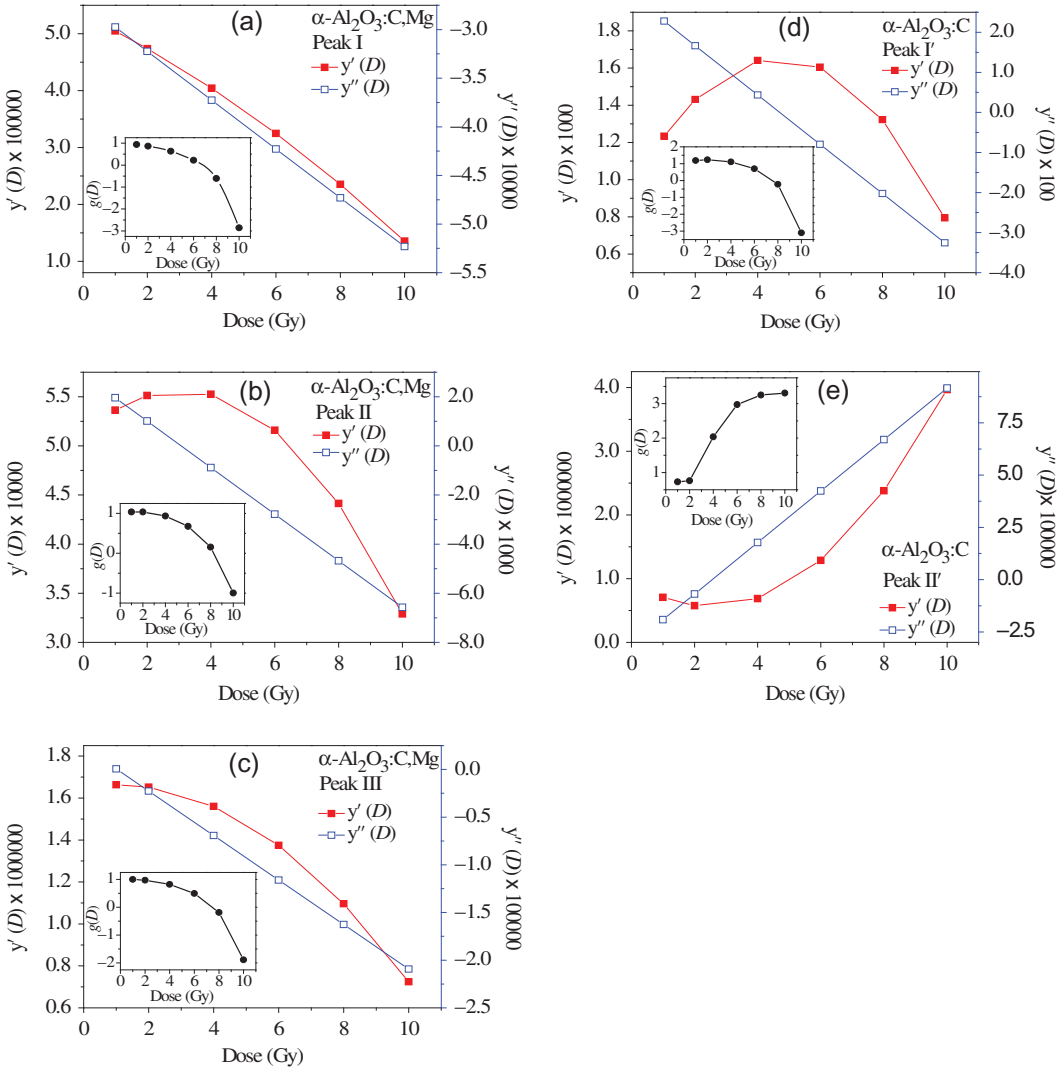


Figure 3. (**a**–**e**) The variation of $y'(D)$, $y''(D)$ and the inset, in each figure, show the variation of $g(D)$ with dose corresponding to peaks I, II and III of α-$Al_2O_3$:C,Mg and peaks I′ and II′ of α-$Al_2O_3$:C, respectively.

$(D)$ as well as $y(D)$ increase with $D$ and $y''(D) > 0$ above 4–10 Gy. Also, $g(D) > 1$ within 4–10 Gy. These results mean that $y(D)$ is superlinear within 4–10 Gy.

The conclusions obtained in the present analysis for the main peak of both α-$Al_2O_3$:C,Mg (peak III) and α-$Al_2O_3$:C (peak II′) are somewhat different from the previous results reported by Kalita and Chithambo[17], Yukihara *et al.*[21] and Chithambo[22]. As stated above, the dose response of the main peak of α-$Al_2O_3$:C,Mg (peak III) is superlinear within 0.1–30 Gy becoming sublinear thereafter up to 100 Gy[17]. On the other hand, the the dose response of the main peak of α-$Al_2O_3$:C (peak II′) is linear within 1–10 Gy, superlinear up to 30 Gy and sublinear above 30 Gy[21, 22]. These apparent differences in the results between the previous[17, 21, 22] and present analyses within 1–10 Gy dose are due to the selection of the dose range. In all the previous analyses[17, 21, 22], a very large dose range (e.g. 0.1–100 Gy[16]) was chosen for analysis. Therefore, the information about the actual nature of the dose response within a short dose range could not be deduced accurately. Moreover, the use of neutral density filter also affects the results as reported in Kalita and Chithambo[17]. Apart from these factors, another important fact is that the sensitivity of

both these samples may change with repeated measurements, which significantly affects the dose response.

## Fading

A TL dosimeter should ideally experience negligible or no fading. Fading is caused by the spontaneous escape of electrons from an electron trap between irradiation and measurement. Kalita and Chithambo[17] studied the fading of the main peak (III) of α-$Al_2O_3$:C,Mg after irradiation to 2 Gy. They reported that the intensity of the peak drops to ~22% of its initial value within 2400 s after irradiation and thereafter to ~14% within 64 800 s. In regards to a material for use as a dosimeter, the fading as observed was high. It was speculated that the fading may be due to the escape of electron from the main trap through the shallow traps by quantum tunnelling[17].

In order to compare fading in α-$Al_2O_3$:C,Mg and α-$Al_2O_3$:C in detail, the loss of intensity of the main peaks (III and II′) as well as the low temperature secondary peaks (I, II and I′) in both the samples were studied.

Figure 4 illustrates fading for the TL in the two materials as described earlier. Figure 4a–c shows the change of the peak intensity (normalised) of peaks I, II and III of α-$Al_2O_3$:C,Mg with storage time for a sample irradiated to different doses (1, 2 and 4 Gy). The data were normalised to the first data corresponding to the measurements made just after irradiation. The same features for peaks I′ and II′ of α-$Al_2O_3$:C are shown in Figure 4d and e. From Figure 4a–c it is evident that the rate of fading of peaks I, II and III of α-$Al_2O_3$:C,Mg depends on irradiation dose. The peaks of α-$Al_2O_3$:C,Mg corresponding to 1 Gy fade faster than those corresponding to 4 Gy. In comparison, no such dose dependent fading of peak I′ and II′ of $Al_2O_3$:C was observed (Figure 4d and e).

The intensity of peak I of α-$Al_2O_3$:C,Mg after 1 and 2 Gy irradiation was found to fade to background level within 300 s. However, the intensity of that peak (peak I) corresponding to 4 Gy took 600 s to fade completely. Further, the intensity of peak II of α-$Al_2O_3$:C,Mg was found to fade completely within 43 200 s for any irradiation dose between 1 and 4 Gy. The intensity of peak II corresponding to 1, 2 and 4 Gy dose after 300 s decreased down to 14, 13 and 12% of the initial intensity, respectively. The main peak (III) of α-$Al_2O_3$:C,Mg was found to fade at a quick rate within 2400 s and after 2400 s the rate of fading decreased. The intensity of peak III after irradiation to 1, 2 and 4 Gy, decreased to 30, 21 and 13%, respectively, within 2400 s; and thereafter, within 2400–64 800 s, the decrease was about 17, 14 and 2%, respectively. On the other hand, peak I′ of α-$Al_2O_3$:C was found to fade completely within 600 s for the sample irradiated to any dose between 1 and 4 Gy. Further, the intensity of the main peak (II′) of α-$Al_2O_3$:C increased with storage time.

The fading in α-$Al_2O_3$:C,Mg and α-$Al_2O_3$:C was analysed in terms of the normalised ratios of the peak intensity against storage time. The general significance of the change of normalised peak ratio (NPR), say, e.g. NPR P2/P1 for peaks P1 and P2 (P1 appears at a lower temperature than P2), with storage time are listed as follows:

(a) If NPR P2/P1 increases, this could be because
    (1) P1 and P2 are distinguishable and either P1 decreases faster than P2 or P2 increases with storage time while P1 remains constant or P2 increases and P1 decreases with storage time.
    (2) P2 is distinguishable but P1 is equivalent to background and P2 increases with storage time.
(b) If NPR P2/P1 decreases, this could be because
    (1) P1 and P2 are distinguishable and either P1 increases faster than P2 or P1 increases while P2 remains constant or P1 remains constant while P2 decreases.
    (2) P2 is distinguishable but P1 is equivalent to background and P2 decreases with storage time.

Figure 5a and b shows the variation of the ratios II/I and III/I corresponding to the peaks I, II and III of α-$Al_2O_3$:C,Mg with storage time whereas Figure 5c shows results for the ratio II′/I′ corresponding to the peaks I′ and II′ of α-$Al_2O_3$:C. Figure 5a indicates that the ratio II/I for α-$Al_2O_3$:C,Mg corresponding to 1 and 2 Gy initially increases in the first 300 s and thereafter decreases up to 64 800 s. Further, for the sample irradiated to 4 Gy, the increase lasts up to 600 s followed by a decrease up to 64 800 s. The increasing and decreasing pattern of the ratio II/I of α-$Al_2O_3$:C,Mg for any doses (1–4 Gy) were found to be similar. The increase of the ratio II/I implies that peak I of α-$Al_2O_3$:C,Mg decreases faster than peak II. However, after 300 s, when the intensity of peak I corresponding to the 1 and 2 Gy irradiated sample drops down to background level and as peak II continues to fade with storage, a decrease in the ratio II/I is observed. The similarity in the variation of the ratio II/I for different dose signifies that the fading process is the same for any dose although the rate of fading differs for different doses.

The ratio III/I of α-$Al_2O_3$:C,Mg is shown in Figure 5b. The increase in the value of III/I signifies that peak I of α-$Al_2O_3$:C,Mg fades quicker than peak III. When the intensity of peak I decreases to background level, the continuous decrease of peak III causes a reduction in the value of III/I. The pattern of increase in the ratio III/I is similar for any dose (1–4 Gy). However, the way the ratio decreases is different for 4 Gy irradiated sample. The slight

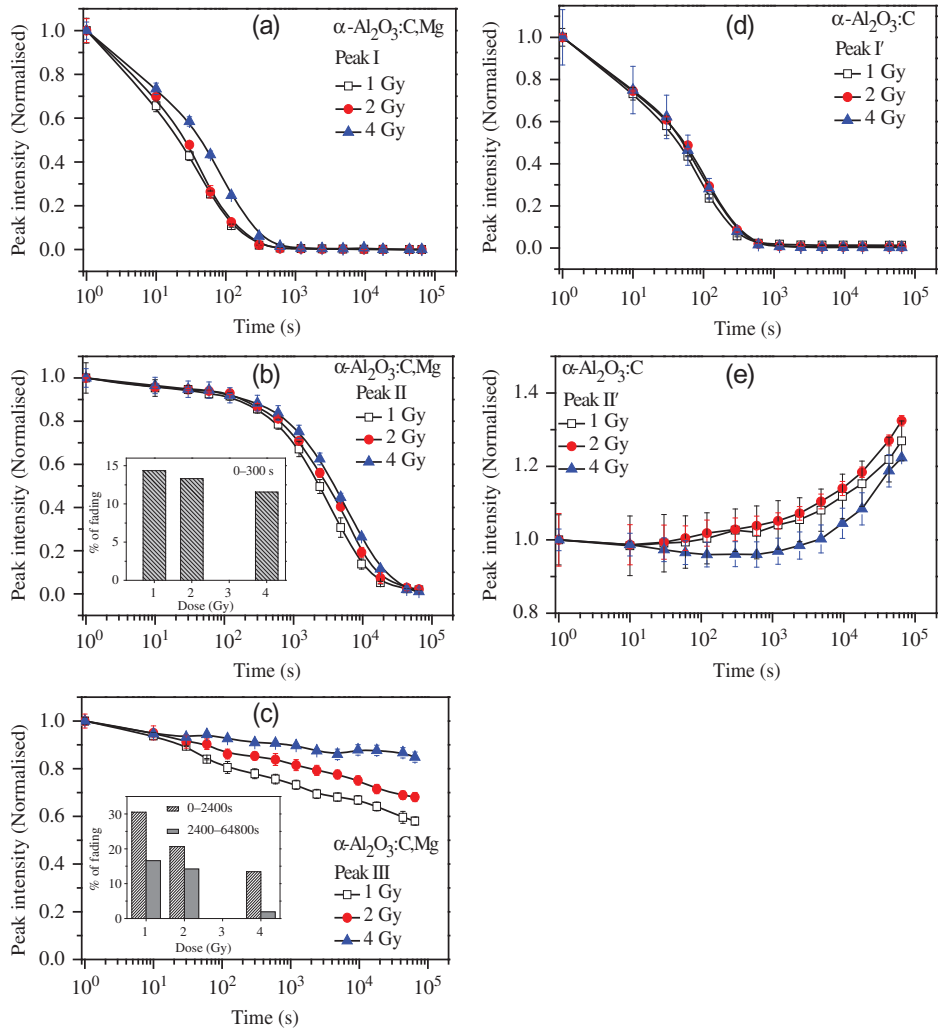


Figure 4. Plots of the normalised peak intensity of peaks as a function of storage for (**a**) peak I, (**b**) peak II and (**c**) peak III of α-$Al_2O_3$:C,Mg and in (**d**, **e**) for peaks I′ and II′ of α-$Al_2O_3$:C. In each plot, the three curves through the data points correspond to the irradiation dose as shown. The inset in (b) and (c) shows the percentage of fading of peaks II and III with storage time.

increase in the ratio seen after 4800 s for the 4 Gy irradiated sample is probably caused by an increase in the intensity of peak III. However, after 18 000 s of delay, the intensity of peak III again decreases. In comparison, the variation of the ratio II′/I′ of α-$Al_2O_3$:C with storage (Figure 5c) shows that II′/I′ increases up to 64 800 s. However, there is an abrupt change at 600 s. This shows that the increase in the ratio II′/I′ up to 600 s is caused by both an increase of peak II′ as well as a decrease of peak I′. However, after 600 s, when peak I′ has faded to background level, the increase in the ratio II′/I′ as shown in Figure 5c is due to the increase of intensity of peak II′ only. It should be noted that the variation of the ratio II′/I′ is independent of irradiation dose. This shows that fading in α-$Al_2O_3$:C is independent of irradiation dose (1–4 Gy). Chithambo and Seneza[19] also found similar results for II′/I′ for measurement corresponding to 0.5 Gy.

This study shows that the main peak (III) of α-$Al_2O_3$:C,Mg fades significantly whereas the main peak (II′) of α-$Al_2O_3$:C shows inverse fading behaviour. As speculated by Kalita and Chithambo[17], the fading mechanism in α-$Al_2O_3$:C,Mg may involve charge tunnelling through the shallow traps. Using kinetic analysis of the glow peaks of α-$Al_2O_3$:C,Mg,

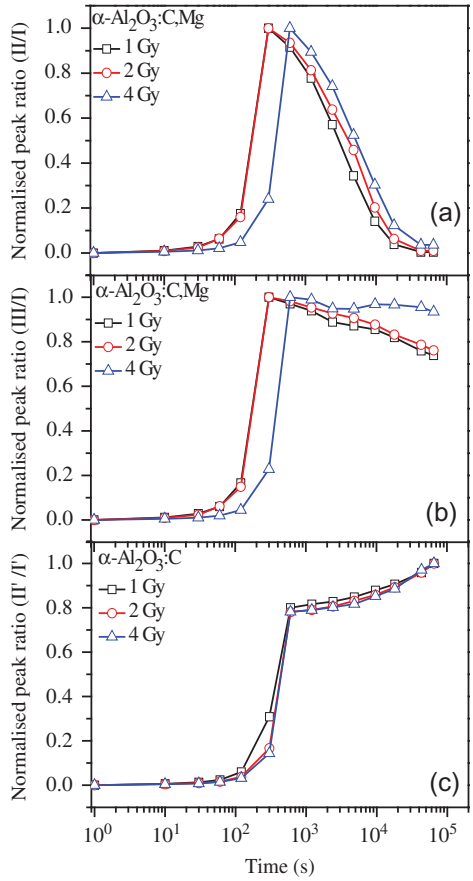


Figure 5. Plots of normalised peak ratio (**a**) II/I, (**b**) III/I and (**c**) II′/I′ with storage time.

we calculated that the activation energy corresponding to peaks I, II, III, IV, V, VI and VII are $E_1 = 0.83$, $E_2 = 0.96$, $E_3 = 1.37$, $E_4 = 1.20$, $E_5 = 1.15$, $E_6 = 1.61$ and $E_7 = 1.94$ eV, respectively[26]. On the other hand, kinetic analysis of the glow peaks of α-$Al_2O_3$:C showed that the activation energy corresponding to peaks I′, II′, IIB′ III′ and IV′ are $E'_1 = 0.72$, $E'_2 = 1.19$, $E'_3 = 0.86$, $E'_4 = 1.15$ and $E'_5 = 1.27$ eV, respectively[20, 27]. In both samples, there are some peaks which appear at relatively higher temperature but with activation energies lower than for some peaks at relatively lower temperatures.

It is notable from the kinetic analysis that in α-$Al_2O_3$:C,Mg, there are seven electron traps with activation energy within 0.83–1.94 eV and that in α-$Al_2O_3$:C, there are five electron traps with activation energy within 0.72–1.27 eV. We summarise that in both samples, charge hopping between the trapping sites at room temperature may be possible due to the presence of such closely spaced trapping sites. Furthermore, both these samples show

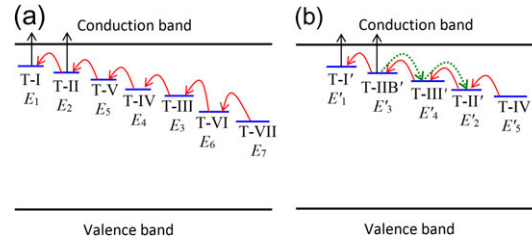


Figure 6. Energy band models for (**a**) α-$Al_2O_3$:C,Mg and (**b**) α-$Al_2O_3$:C to explain the fading mechanism. Here, T-I, T-II…T-VII in (a) represent the trapping sites of α-$Al_2O_3$:C,Mg of activation energy $E_1$, $E_2$ … $E_7$ whereas T-I′, T-II′ …T-IV′ in (b) represent the trapping sites of α-$Al_2O_3$:C of activation energy $E'_1$, $E'_2$ … $E'_4$, respectively. The 'forward' and 'backwards' hopping are represented by the solid curve-arrows and dotted curve-arrows, respectively.

phosphorescence at room temperature[18–20, 26]. This shows that electrons can escape from the shallow traps to the conduction band and subsequently recombine with holes to produce phosphorescence at room temperature. In order to discuss fading in α-$Al_2O_3$:C,Mg and α-$Al_2O_3$:C on the basis of charge hopping and with reference to phosphorescence, two energy band models for α-$Al_2O_3$:C,Mg and α-$Al_2O_3$:C as shown in Figure 6 will be used. The positions of the electron traps T-I, T-II…T-VII and T-I′, T-II′ …T-IV′ in Figure 6 are shown based on the values of their activation energy. In this model, we expect that electrons at electron traps with activation energy less than ~1.00 eV are unstable at room temperature and can escape to the conduction band and subsequently recombine with the holes to produce room-temperature phosphorescence. Apart from this speculation, we also assume that under dark condition and at room temperature, the probability of direct recombination of electrons and holes at any recombination centre without involvement of delocalised band is negligibly small. On this basis, we now discuss the fading of each peak of α-$Al_2O_3$:C,Mg and α-$Al_2O_3$:C.

### *The fading of peak I of α-$Al_2O_3$:C,Mg*

According to the model of α-$Al_2O_3$:C,Mg as shown in Figure 6a, electrons can escape from trap T-I to the conduction band at room temperature since its activation energy (0.83 eV) is low. The fading of peak I is therefore due to the escape of trapped electrons from the trap T-I to the conduction band via which they recombine with holes to produce luminescence. Further, it was observed that when the sample is irradiated to a high dose, peak I takes longer time to fade completely. The dependence of fading on dose may be due to some unspecified dependence of charge hopping rate on the

population of trapped charge. It is reasonable to assume that charge hopping from deeper traps to shallower ones becomes more effective when the population of trapped charge at the deeper electron traps is high. Therefore, when the sample is irradiated to 4 Gy, a greater number of electrons hop to T-I than when the sample is irradiated to 1 Gy. This explains why peak I in a sample irradiated to 1 Gy fades within 300 s whereas when the sample is irradiated to 4 Gy, the intensity of peak I takes longer, at 600 s, to fade completely.

### *The fading of peak II of α-$Al_2O_3$:C,Mg*

The analysis of peak II showed that the peak fades within 43 200 s for any doses (1–4 Gy). However, after the first 300 s when peak I has faded completely, the intensity of peak II was found to decrease down to 14, 13 and 12% of its initial intensity of measurements corresponding to 1, 2 and 4 Gy. The difference in the fading rates of peak II for different irradiation doses may also be explained as has been done for peak I. Charge hopping to T-II from relatively deeper electron traps is prominent when the population of charge at the deeper traps is high. Further, the constant decrease of the intensity of peak II, as discussed with reference to Figure 5a, shows that the reverse charge hopping from T-I to T-II may occur but not to significant extent. Moreover, since the activation energy of trap T-II is <1.00 eV, it follows from our assumption that the loss of intensity of peak II may also be due to escape of the electrons from the trap T-II at ambient temperature to the conduction band and subsequent recombination.

### *The fading of peak III of α-$Al_2O_3$:C,Mg*

The analysis of fading of peak III also suggests the involvement of charge hopping in the process. The activation energy of trap T-III corresponding to peak III is 1.37 eV. At such an energy depth, the trapped electrons are expected to be stable at room temperature. However, as is evident in Figure 4c, the intensity of peak III fades at a high rate. We explain this as being due to the presence of the two nearby traps T-IV and T-V which provide the hopping route for electrons trapped at T-III to reach T-II and T-I. Once the electrons reach the shallower electron traps T-II and T-I, they can escape to the conduction band and thereafter recombine with holes. As for peaks I and II, the rate of fading of peak III was also found to depend on irradiation dose. The rate of fading was high for low irradiation dose compared to the rate of fading for high irradiation dose (Figure 4c). The population of trapped charge at the deeper traps for low dose is less than that in the case of high dose. As a result, the rate of charge hopping (which depends on the population of charge at relatively deeper traps) from the deeper traps T-VI and T-VII to T-III is less for relatively low dose (1 and 2 Gy) irradiated sample. However, for a sample irradiated to 4 Gy, the rate of charge hopping from T-VII to T-VI and subsequently T-VI to T-III increases due to the high population of trapped charge at the deeper traps T-VI and T-VII. As a result, the intensity of peak III was found to increase slightly after 4800 s storage (Figure 4c). On the other hand, the change in intensity of the high temperature secondary peaks (peaks VI and VII) caused by charge hopping cannot be readily studied due to low intensity of the secondary peaks.

Apart from the dose dependent fading behaviour as described above, another significant result is that the rate of fading of peak III in the first 2400 s is very high compared to that in the subsequent 2400 s. This is also due to the dependence of the charge hopping rate on the population of trapped charge at the trapping sites. According to the bar plots shown in the inset of Figure 4c, it may be suggested that the population of trapped charges at the trapping sites after 2400 s reaches a certain level and as such, the rate of charge hopping slows which turn causes the rate of fading to decrease.

### *The fading of peak I′ of α-$Al_2O_3$:C*

According to our working model of α-$Al_2O_3$:C to account for fading as shown in Figure 6b, electrons can escape from the trap T-I′ at room temperature since its activation energy is 0.72 eV. The fading of peak I′ is thus due to the escape of trapped electrons from trap T-I′ to conduction band via which they recombine with holes and give luminescence. Chithambo and Seneza[19] studied the fading as well as phosphorescence of this peak and drew the same conclusion.

### *The fading of peak II′ of α-$Al_2O_3$:C*

The analysis of fading of peak II′ shows that the intensity of this peak increases with storage time independent of irradiation dose. This is inverse fading. In order to discuss this behaviour, we speculate that the charge hopping mechanism we have discussed thus far can take place in two ways: 'forward' meaning from deeper to shallower trap; and 'backwards' from a shallower to a deeper trap. As mentioned earlier, the activation energy of trap T-II′ corresponding to peak II′ is 1.19 eV. Further, kinetic analysis showed that there are two other intermediate traps T-IIB′ and T-III′ with activation energy 0.86 and 1.15 eV, respectively, as illustrated in Figure 6b. The increase of intensity of peak II′ with storage time suggests that the electrons hopping from electron traps T-IIB′ and T-III′ backwards to T-II′ can exceed forward movement from T-II′ to T-III′ and T-IIB′. Moreover, electrons can also come

from T-IV′ to T-II′ in a forward hopping process. Both these movements will tend to increase the population of charge at T-II′ and cause an increase in the intensity of peak II′ with storage time. However, due to the low activation energy of the trap T-IIB′, it is also possible that some electrons can also escape from this electron trap to the conduction band. Unfortunately, due to very low intensity of the high temperature secondary peaks (IIB′, III′ and VI′), no evidence on the change of intensity of these secondary peaks could be properly observed.

## CONCLUSION

A comparative study of the dosimetric features of α-$Al_2O_3$:C,Mg and α-$Al_2O_3$:C relevant to TL dosimetry has been carried out. Analysis showed that the dose response of peaks I (42°C) and III (161°C) of α-$Al_2O_3$:C,Mg is sublinear within 1–10 Gy and that of peak II (72°C) is superlinear within 1–4 Gy followed by a sublinear region within 4–10 Gy. On the other hand, the dose response of peak I′ (48°C) of α-$Al_2O_3$:C is superlinear within 1–4 Gy followed by a sublinear region within 4–10 Gy and that of peak II′ (178°C) is sublinear within 1–4 Gy followed by a superlinear region within 4–10 Gy. Fading analysis showed that the fading in α-$Al_2O_3$:C,Mg was higher than that in α-$Al_2O_3$:C. The rate of fading in α-$Al_2O_3$:C,Mg decreases with increase in dose. However, no such behaviour is observed in α-$Al_2O_3$:C. The fading in both samples has been discussed on the basis of charge hopping that possibly takes place between the trapping sites. From the dose dependence of the fading, it can be concluded that the rate of charge hopping depends on the population of trapped charge at relatively deeper traps.

Regarding the possible routine use of α-$Al_2O_3$:C,Mg and α-$Al_2O_3$:C in TL dosimetry, the change in sensitivity of TL caused by re-use has been studied and it was noted that the sensitivity of these materials changes with re-use[28]. In particular, for α-$Al_2O_3$:C,Mg, that work was carried out using un-annealed and samples annealed at 700 and 900°C. It was noted that for dosimetric application, it is advisable to use TL intensity rather than the area under the TL peak to minimise any errors due to sensitivity change. Further, to minimise any errors associated with sensitivity change, it is advisable to use un-annealed samples for application in TL dosimetry where the sample is re-measured. The suitability of α-$Al_2O_3$:C for dosimetry has been discussed in detail elsewhere[3, 29].

## ACKNOWLEDGEMENTS

J.M. Kalita gratefully acknowledges The Rhodes University Post-Doctoral Research Fellowship (PDF No. s1600221).

## FUNDING

We also appreciate financial support from Rhodes University and the National Research Foundation of South Africa.

## REFERENCES

1. Akselrod, M. S., Kortov, V. S., Kravetsky, D. J. and Gotlib, V. I. *Highly sensitive thermoluminescent anion-defective α-$Al_2O_3$:C single crystal detectors*. Radiat. Prot. Dosim. **32**, 15–20 (1990).
2. Akselrod, M. S. and McKeever, S. W. S. *A radiation dosimetry method using pulsed optically stimulated luminescence*. Radiat. Prot. Dosim. **81**, 167–176 (1999).
3. McKeever, S. W. S., Moscovitch, M. and Townsend, P. D. *Thermoluminescence Dosimetry Materials: Properties and Uses* (England: Nuclear Technology Publishing, Ashford, Kent) (1995) ISBN: 1-870965-19-1.
4. Akselrod, M. S., Larsen, N. A., Whitley, V. and McKeever, S. W. S. *Thermal quenching of F-center luminescence in $Al_2O_3$:C*. J. Appl. Phys. **84**, 3364–3373 (1998).
5. Markey, B. G., Colyott, L. E. and McKeever, S. W. S. *Time-resolved optically stimulated luminescence from α-$Al_2O_3$:C*. Radiat. Meas. **24**, 457–463 (1995).
6. Chithambo, M. L., Nyirenda, A. N., Finch, A. A. and Rawat, N. S. *Time-resolved optically stimulated luminescence and spectral emission features of α-$Al_2O_3$:C*. Physica B **473**, 62–71 (2015).
7. Akselrod, M. S., Akselrod, A. E., Orlov, S. S., Sanyal, S. and Underwood, T. H. New Aluminium Oxide Single Crystals for Volumetric Optical Data Storage (Vancouver, BC, Canada: Optical Society of America) (2003) 10.1364/ODS.2003.TuC3.
8. Akselrod, M. S., Akselrod, A. E., Orlov, S. S., Sanyal, S. and Underwood, T. H. *Fluorescent aluminum oxide crystals for volumetric optical data storage and imaging applications*. J. Fluores. **13**, 503–511 (2003).
9. Akselrod, M. S. and Akselrod, A. E. *New $Al_2O_3$:C,Mg crystals for radiophotoluminescent dosimetry and optical imaging*. Radiat. Prot. Dosim. **119**, 218–221 (2006).
10. Sykora, G. J. and Akselrod, M. S. *Photoluminescence study of photochromically and radiochromically transformed $Al_2O_3$:C,Mg crystals used for fluorescent nuclear track detectors*. Radiat. Meas. **45**, 631–634 (2010).
11. Evans, B. D. and Stapelbroek, M. *Optical properties of the $F^+$ center in crystalline $Al_2O_3$*. Phys. Rev. B **18**, 7089–7098 (1978).
12. Akselrod, M. S., Akselrod, A. E., Orlov, S. S., Sanyal, S. and Underwood, T. H. *New aluminum oxide single crystals for volumetric optical data storage*. Proc. SPIE **5069**, 244–251 (2003).
13. Sykora, G. J., Akselrod, M. S., Salasky, M. and Marino, S. A. *Novel Al2O3:C,Mg fluorescent nuclear track detectors for passive neutron dosimetry*. Radiat. Prot. Dosim. **126**, 278–283 (2007).
14. Akselrod, M. S. and Sykora, G. J. *Fluorescent nuclear track detector technology—a new way to do passive solid state dosimetry*. Radiat. Meas. **46**, 1671–1679 (2011).
15. Eller, S. A., Ahmed, M. F., Bartz, J. A., Akselrod, M. S., Denis, G. and Yukihara, e.g. *Radiophotoluminescence*

*properties of $Al_2O_3$:C,Mg crystals*. Radiat. Meas. **56**, 179–182 (2013).
16. Ahmed, M. F., Schnell, E., Ahmad, S. and Yukihara, e.g. *Image reconstruction algorithm for optically stimulated luminescence 2D dosimetry using laser-scanned $Al_2O_3$:C and $Al_2O_3$:C,Mg films*. Phys. Med. Biol. **61**, 7484–7506 (2016).
17. Kalita, J. M. and Chithambo, M. L. *The influence of dose on the kinetic parameters and dosimetric features of the main thermoluminescence glow peak in α-$Al_2O_3$:C,Mg*. Nucl. Inst. Methods Phys. Res. B **394**, 12–19 (2017).
18. Kalita, J. M. and Chithambo, M. L. *Thermoluminescence of α-$Al_2O_3$:C,Mg: kinetic analysis of the main glow peak*. J. Lumin. **182**, 177–182 (2017).
19. Chithambo, M. L. and Seneza, C. *Kinetics and dosimetric features of secondary thermoluminescence in carbon-doped aluminium oxide*. Physica B **439**, 165–168 (2014).
20. Chithambo, M. L., Seneza, C. and Ogundare, F. O. *Kinetic analysis of high temperature secondary thermoluminescence glow peaks in α-$Al_2O_3$:C*. Radiat. Meas. **66**, 21–30 (2014).
21. Yukihara, e.g., Whitley, V. H., Polf, J. C., Klein, D. M., McKeever, S. W. S., Akselrod, A. E. and Akselrod, M. S. *The effects of deep trap population on the thermoluminescence of $Al_2O_3$:C*. Radiat. Meas. **37**, 627–638 (2003).
22. Chithambo, M. L. *Concerning secondary thermoluminescence peaks in α-$Al_2O_3$:C*. S. Afr. J. Sci. **100**, 524–527 (2004).
23. Kalita, J. M. and Wary, G. *X-ray dose response of calcite—a comprehensive analysis for optimal application in TL dosimetry*. Nucl. Inst. Methods Phys. Res. B **383**, 93–102 (2016).
24. Pagonis, V., Kitis, G. and Furetta, C. Numerical and Practical Exercises in Thermoluminescence (Berlin: Springer) (2006) ISBN: 978-0387-26063-1.
25. Chen, R. and McKeever, S. W. S. Theory of Thermoluminescence and Related Phenomena (Singapore: World Scientific) (1997) ISBN: 9810222955.
26. Kalita, J. M. and Chithambo, M. L. *Comprehensive kinetic analysis of thermoluminescence peaks of α-$Al_2O_3$:C,Mg*. J. Lumin. **185**, 72–82 (2017).
27. Ogundare, F. O., Ogundele, S. A., Chithambo, M. L. and Fasasi, M. K. *Thermoluminescence characteristics of the main glow peak in α-$Al_2O_3$:C exposed to low environmental-like radiation doses*. J. Lumin. **139**, 143–148 (2013).
28. Kalita, J. M. and Chithambo, M. L. *On the sensitivity of thermally and optically stimulated luminescence of α-$Al_2O_3$:C and α-$Al_2O_3$:C,Mg*. Radiat. Meas. **99**, 18–24 (2017).
29. Yukihara, e.g. and Mckeever, S. W. S. Optically Stimulated Luminescence. (Singapore: Wiley) (2011) ISBN: 978-0-470-69725-2.